A simple model of multiple climate regimes

Kerry Emanuel

Program in Atmospheres, Oceans, and Climate, Massachusetts Institute of Technology, Cambridge, Massachusetts, USA

Received 28 June 2001; revised 30 October 2001; accepted 6 November 2001; published 8 May 2002.

[1] Among the most intriguing enigmas of the climate system is that on the one hand, the Earth's climate appears to be exquisitely sensitive to relatively minor variations in the distribution of insolation owing to orbital variations, but on the other hand, it is in a grosser sense stable, in that it has varied only moderately in response to a roughly 30% increase in solar insolation over the life of the planet. To this enigma may be added the evidence that climate may undergo extraordinarily abrupt transitions. An attractive idea to help explain these characteristics is the notion that the Earth possesses a limited number of stable climate regimes that may overlap to produce multiple equilibrium states for the same solar forcing. Here we present a simple model that produces such overlapping stable equilibria, based on a few key feedback processes. These include control of atmospheric clouds and water vapor by the large-scale circulation of the atmosphere, control of the depth and intensity of the ocean's thermohaline circulation by tropical cyclones, and the dependence of atmospheric CO_2 content on ocean temperature and the strength of the thermohaline circulation. We will show that these key feedback processes produce a climate with two or three stable, overlapping climate regimes. Subjecting this system to variations in climate forcing can account for several observed features of the climate system, including abrupt transitions, sensitivity to orbital variations, arctic warmth and high bottom water temperature during the Eocene and late Cretaceous, tempestites, and possible episodes of deep ocean anoxia during the Cretaceous. *INDEX TERMS:* 1610 Global Change: Atmosphere (0315, 0325); 1620 Global Change: Climate dynamics (3309); 1615 Global Change: Biogeochemical processes (4805); 1625 Global Change: Geomorphology and weathering (1824, 1886); *KEYWORDS:* paleoclimate, hurricanes, Eocene warmth, thermohaline, climate regimes

1. Introduction

[2] It has become increasingly apparent that climate change is often abrupt, occurring on timescales very short compared to the duration of climate regimes, such as glacials and interglacials [e.g., see *Adams et al.*, 1999]. While there is a strong correlation between orbital cycles and climate change [*Imbrie*, 1985], the orbital forcing is periodic while the climate response is marked by very sudden regime shifts. To add to this mystery, the magnitude of the orbital cycle-induced changes in the latitudinal distribution of insolation is quite small. If the observed climate response to these variations were extrapolated to the much larger changes in insolation accompanying changes in solar luminosity since the inception of the solar system, the resulting climate change would be excessive. Thus the earth's climate appears to be exquisitely sensitive to small variations in forcing, but rather insensitive to large variations.

[3] An attractive idea that would account for this behavior is the notion that the climate system possesses a limited number of possibly overlapping regimes, so that small changes in forcing may effect abrupt transitions between regimes, but even large variations of forcing cannot drive the system off the collection of states comprised by the set of regimes.

[4] The idea that the climate system may have discrete regimes dates back at least to the work of *Chamberlin* [1906], who suggested that the oceans' thermohaline circulation may exist in a alternate state, in which warm, salty water sinks in the subtropics and flows poleward at depth. (Some doubt has been cast on this possibility by the recent work of *Bice and Marotzke* [2001].) More recent work by *Broecker et al.* [1985], *Manabe and Stouffer* [1988], and *Marotzke and Willebrand* [1991] suggests that the thermohaline circulation may possess several stable configurations for the same forcing. That variations in the thermohaline circulation are associated with global climate change is supported by the work of *Boyle and Keigwin* [1987], *Keigwin et al.* [1991], *Lehman and Keigwin* [1992], and *Rind and Chandler* [1991], among others.

[5] The possibility that climate is quantized is suggested by the work of *Paillard* [1998], who showed that an extremely simple quantum climate model, with a minimum number of rules on state transitions, is capable of accounting for many of the most important climate changes over the last million years, when forced by orbitally determined insolation at high latitudes. While the model is largely devoid of physics, it does suggest that the climate response to periodic forcing is more nearly that of a quantum system than of a linear system.

[6] Of particular interest among documented climate regimes is the early Eocene (50–55 Ma), during which high latitudes were 10–15 K warmer than present while tropical temperatures were not much different [*Zachos et al.*, 1994], or perhaps 2–4 K warmer than present [*Pearson et al.*, 2001]. Very large poleward heat transport by the oceans and/or atmosphere is almost certainly necessary to explain the polar warmth of this period, though it may not be sufficient. General circulation modeling of the atmosphere [e.g., *Huber and Sloan*, 1999; *Rind and Chandler*, 1991] does not support the idea that there can be substantially greater poleward heat flux in the face of greatly diminished temperature gradients, pointing to the oceans as the likely source of the increased transport. Most efforts to explain increased oceanic heat flux in the presence of diminished temperature gradients have focused on increased driving by salinity gradients, but the work of *Bice and Marotzke* [2001] casts serious doubts on this possibility.

[7] The present work is motivated by the idea, dating back to *Sandstrom* [1908], that the magnitude of heat transport by the

0148-0227/02/2001JD001002$09.00

ocean is limited by vertical mixing. If the vertical mixing is itself a strong function of the climate state, then increased mixing in warm climates could conceivably yield large poleward heat transport, even in the face of diminished meridional temperature gradients. In a recent paper [*Emanuel*, 2001], the author presented evidence that global tropical cyclone activity contributes much of the vertical mixing that drives the oceans' thermohaline circulation. Under the reasonable expectation that tropical cyclone activity is enhanced in warmer climates, one might expect increased mixing of the upper ocean and increased poleward heat transport by the ocean to result.

[8] This paper explores the possible implications for global climate of the dependence of oceanic heat transport on global tropical cyclone activity, using a highly simplified model of the climate system. The essential feedback processes included in this model are described in section 2, while a description of the model itself may be found in section 3. The results are presented in section 4, while section 5 contains a concluding discussion.

2. Essential Climate Feedback Processes

[9] The theory of multiple climate regimes presented here depends on three key feedback processes involving the atmosphere, oceans and the global carbon cycle. In section 3, we will construct a model of the climate system based on these feedback mechanisms. The novel feedback upon which everything else depends is the driving of the deep overturning circulation of the ocean, which we therefore present first.

2.1. Driving of the Ocean's Thermohaline Circulation

[10] The world's oceans carry roughly one third of the net equator-to-pole heat flux necessary to balance the satellite-observed meridional distribution of net radiative flux at the top of the atmosphere [*MacDonald and Wunsch*, 1996] and thus play a critical role in setting the global temperature distribution. Of this third, a substantial fraction is thought to be carried by the deep, meridional overturning circulation (hereafter denoted MOC) with the rest carried by the wind-driven lateral gyres in the principal ocean basins [*Hall and Bryden*, 1982; *Wang et al.*, 1995].

[11] A fundamental problem in the physics of the deep overturning of the ocean was first identified by *Sandstrom* [1908]. Aside from a minor contribution by geothermal heating, there are essentially no internal heat sources or sinks in the world oceans, with all of the heat entering and leaving through the top surface. Thus, without some other effect, there can be no conversion of thermal to mechanical energy, as the oceans' heat engine is operating at zero thermodynamic efficiency. To overcome this problem, *Jeffreys* [1925] suggested that turbulence could mix relatively warm water into colder water at depth, thus introducing an enthalpy source at relatively high pressure, resulting in a circulation in which buoyancy plays an active role. In this view, the rate of overturning is, in the long run, controlled by the rate of downward diffusion of enthalpy, as reviewed by *Munk and Wunsch* [1998], who estimated that $2.1 \times 10^{12} W$ must be expended in turbulent mixing to explain the estimated 30 Sv of global deep water formation.

[12] Three particular aspects of this mechanism are noted here. First, to be effective, the turbulent mixing must occur on the warm side of the system; mixing in regions of deep water formation has little or no effect [*Marotzke and Scott*, 1999]. Second, to explain the steady state ascent of water through isopycnal surfaces, there must be a net, vertically integrated density sink, and this requires that the mixing ultimately communicate with the surface. Mixing that is purely internal to the ocean and does not affect the surface density cannot cause a vertically integrated density source and leads instead to the formation of internal mixed layers. Third, the required mixing can be highly localized in space (J. R. Scott and J. Marotzke, personal communication, 2000) and, perhaps, in time as well.

[13] The author [*Emanuel*, 2001] has suggested that the source of mixing required to drive the thermohaline circulation is provided by global tropical cyclone activity. Tropical cyclones are observed to strongly mix the upper ocean, resulting in prominent cold wakes. The recovery of those wakes, which is observed to occur over a period of 2–3 weeks, represents a net heat flux into the sea surface that must, in the long run, be balanced by lateral export by the ocean. Using records of all tropical cyclones that occurred globally during 1996, together with simulations of all of those storms using a simple, coupled ocean-atmosphere tropical cyclone model, he was able to estimate that the lateral oceanic heat flux induced by global tropical cyclone activity is $1.4 \pm 0.7 \times 10^{15} W$, comparable to the observed poleward heat flux by the oceans as estimated by *MacDonald and Wunsch* [1996].

[14] Basic scaling arguments as well as numerical simulations with an ocean model (J. R. Scott and J. Marotzke, personal communication, 2001) suggest that the lateral heat flux induced by a source of mixing in the tropical oceans scales as

$$F \sim P^{2/3} B^{2/3} \tag{1}$$

where F is the lateral heat flux by the ocean, P is the power expended in vertical mixing, and B is the total buoyancy gradient at the sea surface. Thus heat transport by the deep ocean circulation is as sensitive to vertical mixing as it is to the meridional temperature gradient. If indeed the main source of vertical mixing is tropical cyclone activity, it follows that changes in tropical cyclone activity can force changes in the poleward heat flux by the oceans and thereby affect climate. It is the thesis of the present paper that the response of global tropical cyclone activity to climate change constitutes an essential feedback in the climate system. Such a feedback is absent from all current global climate models. We shall use (1) as a key component in the simple box model of the climate system described in section 3.

2.2. Greenhouse Trapping and the Large-Scale Circulation of the Atmosphere

[15] Satellite imagery clearly shows that much of the longwave radiation leaving the planet does so through large-scale patches of dry, cloud-free air that occur primarily in the subtropics [*Pierrehumbert*, 1995]. These are regions where air is descending in association with large-scale atmospheric circulation systems, such as the Hadley and Walker cells. Recent work [e.g., *Spencer and Braswell*, 1997] shows that the air in such regions is about as dry as air descending without mixing from the tropical tropopause, down to the top of the trade wind boundary layer.

[16] The air is exceedingly dry in these regions because the large-scale downward motion is sufficient to prevent deep moist convection. Experiments with a two-column model by *Nilsson and Emanuel* [1999] show that if the strength of the large-scale circulation falls below a critical threshold, deep convection will occur in the descent region of the large-scale circulation, albeit not with the level of activity found in the ascent region. When this happens, the descent region becomes substantially more humid than when deep convection is absent, though it is still drier than the ascent region. At the same time, the ascent region becomes drier as the intensity of the large-scale circulation wanes, but the changes in relative humidity are far less dramatic than those that take place in the descent region. This, coupled with the nonlinear dependence of longwave absorption on relative humidity [*Schneider et al.*, 1999], implies that the net greenhouse trapping by the atmosphere increases considerably as the strength of the large-scale circulation falls below that necessary to suppress deep convection in the descent regions.

[17] As we shall attempt to demonstrate, in section 3 below, there may exist climate regimes in which the strength of the heat transport by the ocean is so large as to render the meridional temperature gradient of the atmosphere too small to support strong,

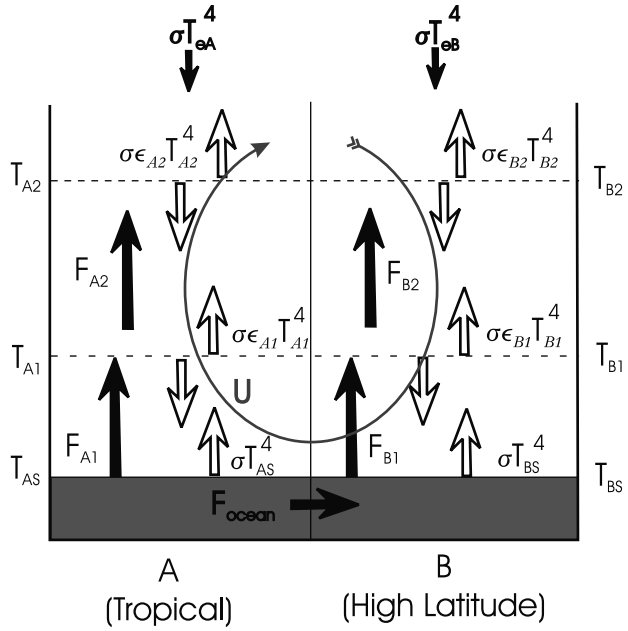

Figure 1. Model structure. Insolation is represented by effective blackbody emission temperatures, as indicated at top. Temperature is defined at the sea surface and two atmospheric layers, in each of two boxes corresponding to low and high latitude. Infrared fluxes denoted by white arrows, while black arrows show convective fluxes and ocean flux.

large-scale circulation. When this happens, the infrared windows through which longwave radiation escapes to space from the surface and low levels of the atmosphere close and the greenhouse trapping by the atmosphere becomes somewhat greater.

2.3. Atmospheric CO_2 and the Thermohaline Circulation

[18] Ice cores collected in Greenland and Antarctica show that atmospheric carbon dioxide content varied synchronously with measures of temperature and ice volume (e.g., see *Sigman and Boyle* [2000] over at least the last 450,000 years. While there is no generally accepted explanation for this, several different mechanisms have been elucidated. Air-sea exchange of CO_2 is determined largely by the partial pressure of CO_2 in surface waters, which is in turn determined by temperature and the chemical composition of the ocean. CO_2 is more soluble in cold, fresh water than in warm, salty water. Thus changes in the temperature distribution of the ocean could affect the balance between the atmosphere and ocean, the latter of which contains nearly 60 times the carbon content, in the form of dissolved inorganic carbon, as the atmosphere. In particular, deepening of the tropical thermocline, all other things being equal, will increase the volume of relatively warm water in the ocean and thereby take some dissolved CO_2 out of solution, increasing atmospheric CO_2. According to the scaling found by J. R. Scott and J. Marotzke (personal communication, 2001), the thermocline depth is related to mixing and buoyancy differential by

$$h \sim P^{1/3} B^{-2/3}, \tag{2}$$

where h is the thermocline depth. Thus all other things being equal, one might expect atmospheric CO_2 content to increase slowly with the power expended in mixing and more rapidly as the buoyancy gradient at the ocean surface decreases.

[19] This is only part of the oceanic influence on atmospheric CO_2. As reviewed by *Sigman and Boyle* [2000], the response of atmospheric CO_2 to climate change is complex and depends on several factors beyond ocean temperature and circulation change. These factors include interaction with the continental biosphere, changes in oceanic alkalinity, and nutrient supply and utilization. Here we simply point out that mixing-induced changes in ocean circulation may be expected to have potentially large effects on atmospheric CO_2 through a complex set of mechanisms. In the simplified model to be discussed presently, we shall assume, as a first step, that atmospheric CO_2 varies with the volume-weighted mean temperature of the ocean. As we shall see, cold oceans are generally associated with strong atmospheric circulation, which might be expected to increase the supply of continental dust to the oceans, thereby "fertilizing" the upper ocean, increasing primary productivity, and reducing atmospheric CO_2. This works in the same direction as our assumption that atmospheric CO_2 varies in proportion to mean temperature.

3. A Simple Climate Model

[20] As a first step in examining the effect of the climate feedbacks discussed in the previous section, we construct a simple, two-box climate model consisting of a two-layer atmosphere and a single ocean layer, as illustrated in Figure 1. The left-hand box (box "A") covers the tropics, while the right-hand box (box "B") represents higher latitudes. The surface is assumed to have an emissivity of unity, while each of the atmospheric layers has longwave emissivity $\varepsilon_{i,j}$, where the index i refers to either box A or box B, and the index j refers to level 1 or 2. These emissivities depend on water vapor and CO_2 content, as described below. The atmosphere is assumed to be entirely transparent to incoming shortwave radiation, which is characterized by the effective blackbody emission temperatures T_{eA} and T_{eB} in boxes A and B, respectively.

[21] Turbulent fluxes carry enthalpy from the surface to the first layer, and from the first to the second layer in each box. These fluxes are determined so as to enforce the condition that the temperature lapse rate be no larger than moist adiabatic lapse rates. That is, we enforce the condition that

$$T_{i,j} \le T_{i,j+1} + \Delta T_{i,j}, \tag{3}$$

where the index i refers to either box A or box B, and the index j refers to either the surface (s) or level 1. The temperature differences, $\Delta T_{i,j}$, are determined from saturated adiabats corresponding to temperature $T_{i,j}$. If the solution without turbulent fluxes satisfies equation (3), then it is assumed that there are no turbulent fluxes in that layer and box. If, on the other hand, equation (3) is violated, just enough turbulent flux is brought to bear to enforce the equality of the left and right sides of equation (3). In practice, we do this by representing the turbulent fluxes as

$$F_{i,j} = \beta\left(T_{i,j} - T_{i,j+1} - \Delta T_{i,j}\right), \tag{4}$$

where β is a large number and $F_{i,j} \ge 0$ is enforced.

[22] A large-scale atmospheric circulation is assumed to transport heat from box A to box B. This is accomplished by a combination of horizontal advection of enthalpy and vertical advection of static energy. As in the case of the vertical fluxes, the horizontal circulation is determined to enforce the condition that a measure of the horizontal temperature gradient not exceed some critical value. This is a good approximation to heat transport by the Hadley circulation in the Tropics, as elucidated, for example, by *Held and Hou* [1980], who showed that such circulations tend to keep the actual temperature gradient close to a critical value that depends on latitude and the angular rotation rate of the earth. More recently, *Emanuel* [1995] showed that in a moist atmosphere, Hadley circulations act to keep the meridional gradient of moist entropy close to a similarly determined critical

value. In this simple model, the moist entropy gradient in the boundary layer will be nearly proportional to the horizontal gradient of the top layer temperature, if the vertical lapse rate is moist adiabatic. Thus we determine the magnitude of the circulation by

$$U = \beta(T_{A2} - T_{B2} - \Delta T_c), \tag{5}$$

where once again β is a large number, ΔT_c is a critical horizontal temperature gradient, and we enforce $U \geq 0$, so that there is no atmospheric circulation if the temperature gradient is below a threshold value. Once the circulation is obtained, the meridional enthalpy transport is calculated using upwind differencing, as shown in the Appendix.

[23] While there is some justification for this approach as applied to heat transport by the tropical circulation, there is less justification for its application to higher latitudes, where the heat transport is dominated by baroclinic eddies. Nevertheless, such eddies do act to transport enthalpy down its mean gradient, so a formulation like equation (5) is qualitatively correct, though the coefficient β is not necessarily large and the actual transport is more nearly proportional to a higher power of the horizontal temperature gradient. In keeping with the simplicity of the present model, and as we cannot make a distinction between tropical and extratropical enthalpy transport in the present model structure, we shall apply equation (5).

[24] The emissivities of each atmospheric layer are based on the concentrations of CO_2 and water vapor in those layers. Treating each atmospheric layer as a gray body absorber and emitter, the emissivities of each layer and box are given by

$$\varepsilon_{i,j} = 1 - e^{-\alpha \mathrm{CO}_2 - \gamma q_{i,j}}, \tag{6}$$

where CO_2 is the atmospheric CO_2 content, $q_{i,j}$ is the specific humidity of box i and layer j, and α and γ are constant coefficients. This represents a crude approximation to the transmittance function [e.g., see *Goody and Yung*, 1995] but is appropriate given the crude vertical structure of the model. The specific humidities, $q_{i,j}$, are given by their saturation values at the appropriate temperature, multiplied by a constant relative humidity (which can be absorbed into the definition of γ). An exception to this rule is applied in the upper layer of box B, where the relative humidity decreases with increasing circulation strength, vis.

$$q_{B2} = \mathrm{H}\, q^*_{B2}(1 - aU), \tag{7}$$

where H is the prescribed background relative humidity, q^*_B,2 is the saturation specific humidity of level 2 in box B, and a is a constant. The specific humidity given by equation (7) is not permitted to be negative. This formulation allows for the drying effect of large-scale subsidence, as discussed in section 2.2, and constitutes a positive feedback in this model.

[25] Although atmospheric CO_2 content is in reality a complex and poorly understood function of many variables, including volcanic outgassing, terrestrial biology, ocean circulation, ocean temperature and ocean primary productivity, which in turn depends on the supply of oxygen and nutrients, we model it here as a simple function of mass weighted ocean temperature:

$$\mathrm{CO}_2 = C + \lambda\left(T_{BS} + \frac{h}{H}(T_{AS} - T_{BS})\right), \tag{8}$$

where C is a base value of CO_2 and can represent the effects of other invariant trace gases as well, λ is a constant, h is given by equation (2), whose precise formulation will be given presently, and H is some mean ocean depth. Although this formulation omits many important influences on CO_2, it does account loosely for the effect of CO_2 solubility in surface waters. The parameters in equation (8) are tuned to give reasonable fluctuations of CO_2 between glacial and interglacial climates. We shall return later to a discussion of the possible influence of omitted processes on the behavior of the model.

[26] To close the model, we need expressions for the oceanic heat flux and the tropical thermocline depth, which is used in equation (8). These are given by equations (1) and (2). In these expressions, we take the buoyancy gradient between the tropical and high-latitude ocean boxes to be

$$B \sim T_{AS} - T_{BS}, \tag{9}$$

while the mixing power is related to tropical cyclone activity by

$$P \sim \sum_i V_i^3, \tag{10}$$

where V_i is a characteristic maximum wind speed in tropical cyclones and the sum is taken over the globe and some characteristic averaging time. Variations in the mixing power provided by global tropical cyclone activity will be owing to variations in the strength of individual storms and variations in the overall frequency of events. Unfortunately, little is known about climatic control of tropical cyclone frequency [*Henderson-Sellers et al.*, 1998]. On the other hand, there is a strong statistical relationship between average storm intensity, as measured by maximum wind speeds, and the theoretical upper bound on storm intensity [*Emanuel*, 2000]. This theoretical bound, called the potential intensity, is given by *Bister and Emanuel* [1998] and may be expressed approximately as

$$V_i^2 \sim \varepsilon_T(k_0^* - k), \tag{11}$$

where k_0^* and k_0 are the saturation enthalpy of the sea surface and the actual enthalpy of the unperturbed boundary layer air, respectively, and ε_T is a thermodynamic efficiency, proportional to the difference between the sea surface temperature and the temperature at the top of the moist convecting layer, assumed to be the tropopause in the Tropics. We here assume that tropical cyclones occur only in the Tropics, and that the thermodynamic efficiency, ε_T, is a constant *unless* the deep convective flux in box A, F_{CA}, vanishes, in which case we assume that there is insufficient thermodynamic efficiency to sustain tropical cyclones and set $\varepsilon_T = 0$.

[27] We determine $(k_0^* - k)$ in equation (11) by working backward through the aerodynamic flux formula for the surface flux of enthalpy under unperturbed conditions:

$$F_{A1} \sim |V_s|(k_0^* - k), \tag{12}$$

where $|V_s|$ is a characteristic magnitude of the surface wind speed. We take this speed to be given by

$$|V_S| = \sqrt{u_*^2 + U^2}, \tag{13}$$

where U is the explicit circulation strength and u_* accounts for the contribution of small scale and fluctuating wind to the average wind speed. Combining equations (11)–(13), we get

$$V_i^2 \sim \varepsilon_T \frac{F_{A1}}{\sqrt{u_*^2 + U^2}}. \tag{14}$$

[28] This, coupled with equation (10), gives the mixing power that is used to drive the ocean heat flux using equations (1) and (9), and the tropical thermocline depth given by equations (2) and (9).

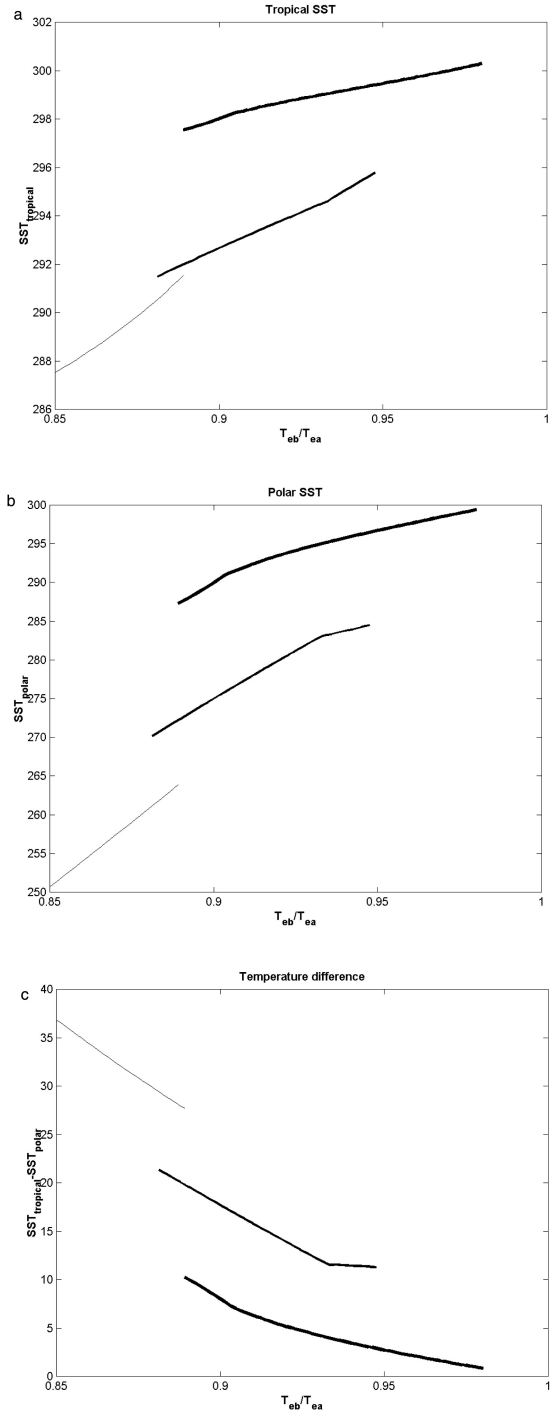

Figure 2. Steady equilibrium temperature as a function of the ratio of high- to low-latitude insolation. In each figure, the thin line shows the cold regime solution, the medium line shows the moderate regime, and the thick line shows the hot regime. (a) Low-latitude temperature, (b) high-latitude temperature, and (c) their difference.

[29] This completes the model formulation. A summary of the model equations together with the constants used in most of the integrations is given in the Appendix. The time-dependent equations are integrated forward in time until a steady state is achieved. For each set of forcings, this integration is performed for multiple initial conditions, in case there are multiple (stable) equilibria. In the solutions discussed presently, the forcing is varied primarily by changing the insolation to (as represented by the effective emission temperature of) box B, but there are other choices, such as altering the base state CO_2 given in equation (8).

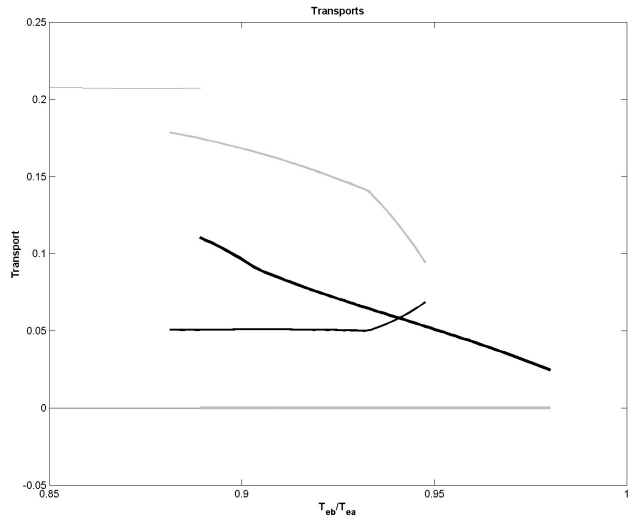

Figure 3. As in Figure 2, but showing nondimensional lateral enthalpy transport. Gray lines show atmospheric transport; black lines show oceanic transport.

4. Results

4.1. Standard Run

[30] The box model described in the previous section usually produces two or three stable regimes, depending on the choice of parameters. For the parameters given in the Appendix, the solutions fall into three partially overlapping stable regimes, as demonstrated by Figure 2, which shows the surface temperature in the low- and high-latitude boxes, and their difference. These solutions are shown as a function of the ratio of the effective black body emission temperatures of the high- and low-latitude boxes, a measure of the latitudinal gradient of insolation. The absolute values of the temperature should not be taken too seriously, given the crude nature of the model. Note that the jumps in the polar surface temperature are considerably greater than those of the tropical surface temperature, owing partially to the water vapor feedback, which affects the polar temperatures more, and, in the case of the jump from the "cold" to the "moderate" solution, to the jump in poleward enthalpy transport, whose behavior is displayed in Figure 3. In the cold solution, all the poleward heat flux is carried by the atmosphere. The atmospheric overturning is so vigorous in this regime that its cooling of the lower tropical atmosphere stabilizes the column so that there is no convective flux from the first to the second layers of the tropical box and thus no tropical cyclones to drive the ocean mixing. In the moderate regime, the poleward heat flux is carried by both the atmosphere and oceans, while in the "hot" regime, the ocean's heat transport is so effective that it drives the atmospheric temperature gradient subcritical, shutting down the atmospheric circulation.

[31] Note that the total poleward enthalpy transport (Figure 3) is largest in the moderate regime solution. In the cold solution, the ocean heat transport is absent, while in the hot regime, the high-latitude atmosphere is sufficiently opaque that little heat transport is required; moreover, there is no poleward heat flux by the atmosphere. The strength of the atmospheric overturning is shown in Figure 4.

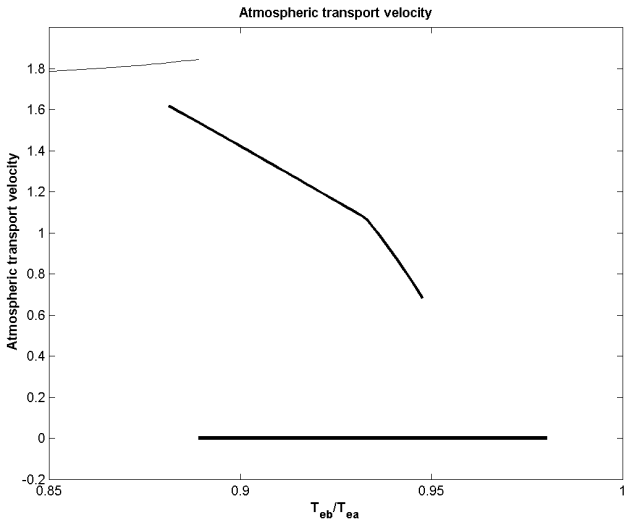

Figure 4. As in Figure 2, but showing nondimensional atmospheric transport velocity.

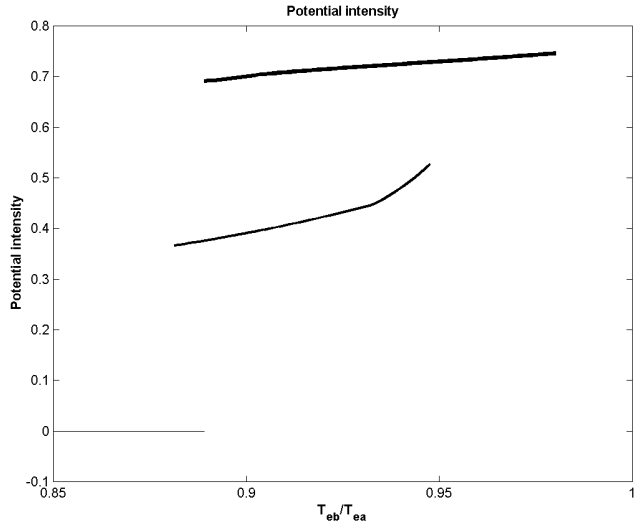

Figure 6. As in Figure 2, but showing the nondimensional potential maximum wind speed of tropical cyclones in the low-latitude box.

[32] Vertical heat fluxes in the tropical box are shown in Figure 5. Surface fluxes are comparable in all regimes, but the convective flux from the bottom to the top layer varies strongly, being completely absent in the cold regime. Here the atmospheric overturning is so strong that it stabilizes the tropical atmosphere to deep convection. One consequence of this, that has not been included in the present model, is that the upper tropical troposphere is likely to be much drier, as there is no means by which it could be moistened. This would make the cold solution even colder.

[33] The potential intensity of tropical cyclones is displayed in Figure 6. The absence of deep convection prevents tropical cyclone activity in the cold regime. The jump in potential intensity from the moderate to the hot regime is primarily owing to a decrease in the mean surface winds, per equation (14). The large tropical cyclone activity in the hot regime solution maintains a vigorous poleward heat flux by the ocean, in spite of a weak lateral temperature gradient.

[34] The emissivity of the upper layer of the high-latitude box is shown in Figure 7. The small jump from the cold to the moderate regime is owing mostly to the temperature dependence of the water vapor content but also, in part, to a decrease in the vigor of subsidence associated with the atmospheric overturning and to an increase in carbon dioxide content stemming from the change in ocean temperature, via equation (8). The large jump from the moderate to the hot regime has contributions from these two effects, but is dominated by the cessation of atmospheric circulation and attendant subsidence drying.

[35] Figure 8 shows the depth of the tropical thermocline. In the cold regime, the thermocline approaches the surface as, in this model, there is no vertical mixing when tropical cyclones are absent. In the moderate regime, the thermocline depth slowly increases with a reduction in the latitudinal gradient of insolation, owing to an increase in tropical cyclone potential intensity and to the reduction of the meridional gradient of ocean temperature (see equation (2)). There is a large increase in the thermocline depth in the hot regime,

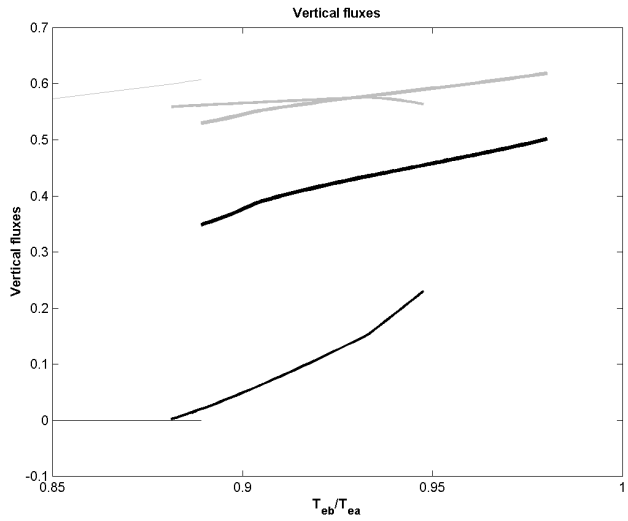

Figure 5. As in Figure 2, but showing turbulent vertical fluxes in the low-latitude box. Gray lines show fluxes from level 1 to level 2; black lines show surface fluxes.

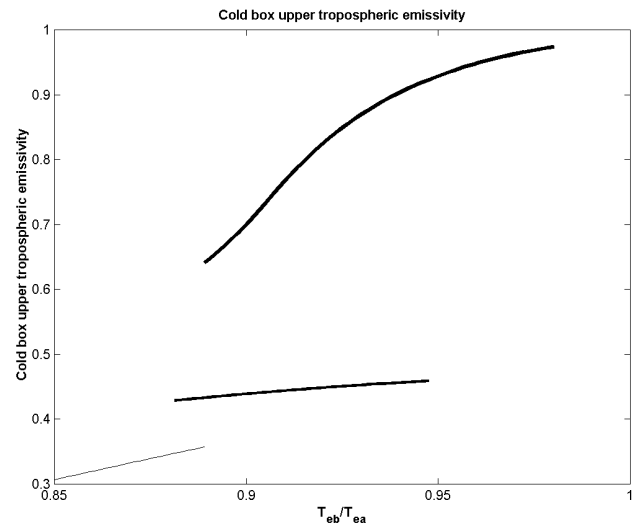

Figure 7. As in Figure 2, but showing the emissivity of layer 2 in the high-latitude box.

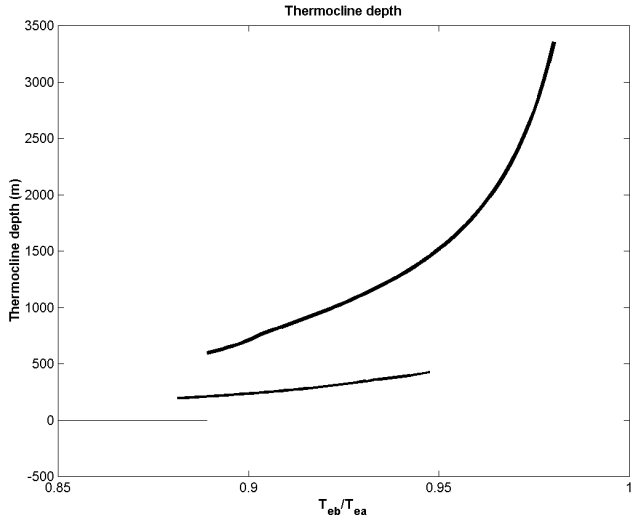

Figure 8. As in Figure 2, but showing the tropical thermocline depth.

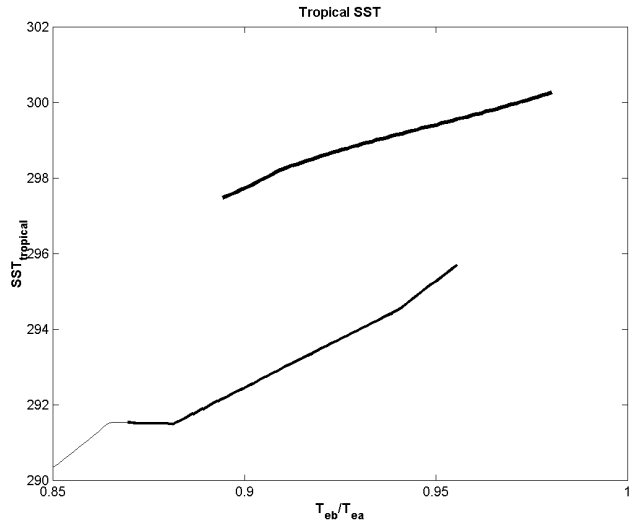

Figure 10. As in Figure 2a, except that atmospheric CO_2 constant.

since the meridional gradient of ocean temperature becomes very weak while the intensity of tropical cyclones becomes large.

[36] Finally, the atmospheric CO_2 content is displayed in Figure 9. The largest jump in CO_2 is from the cold to the moderate regime. Given the uncertainty in how atmospheric carbon dioxide responds to long-term changes in the thermohaline circulation and ocean temperature, this must be viewed as highly uncertain. However, the discontinuous transition between the cold and moderate regimes in this model does depend on the presence of CO_2 feedback, as shown in Figure 10, in which the atmospheric CO_2 content has been fixed at 280 ppm. Now the temperature varies continuously between the cold and moderate regimes. We note, however, that there is no ice-albedo feedback in this simple model; the effects of such a feedback are likely to be at least as strong as the order 100 ppm jump in CO_2 between the cold and moderate regimes. Experiments with a simple ice scheme relating the albedo of the high-latitude box to its temperature show that the third (cold) regime can be restored with the albedo feedback, even in the absence of CO_2 feedback.

[37] Depending on the choice of parameters, the model does not always achieve a steady state. For example, in Figure 10, no true steady state exists for T_{eb}/T_{ea} between about 0.86 and 0.88. (The solution shown represents an average of the time-dependent solution.) In these cases, the solution "flip-flops" between two quasi-equilibrium states, with the timing of the transitions being either periodic or chaotic.

4.2. Sensitivity to Parameters

[38] As indicated in the Appendix, even a simple model like the one presented here has an impressive number of parameters, such as the assumed relative humidity of the troposphere, the relationship between hurricane potential intensity and ocean mixing, the base value of the CO_2 content, etc. Given that the present study is only a starting point, we have not undertaken an exhaustive study of the sensitivity of the model to all of the parameters. Broadly, a sufficient variation of any parameter that affects the pole-to-equator temperature gradient will produce two or three regimes, as long as the value of the other parameters do not overwhelming favor one

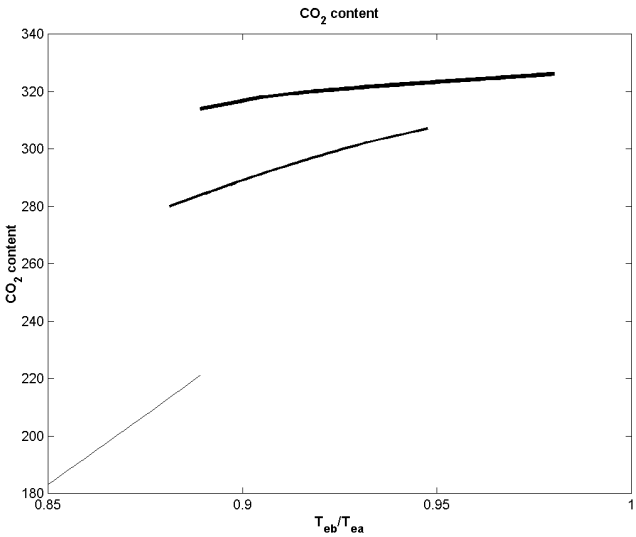

Figure 9. As in Figure 2, but showing the atmospheric CO_2 content.

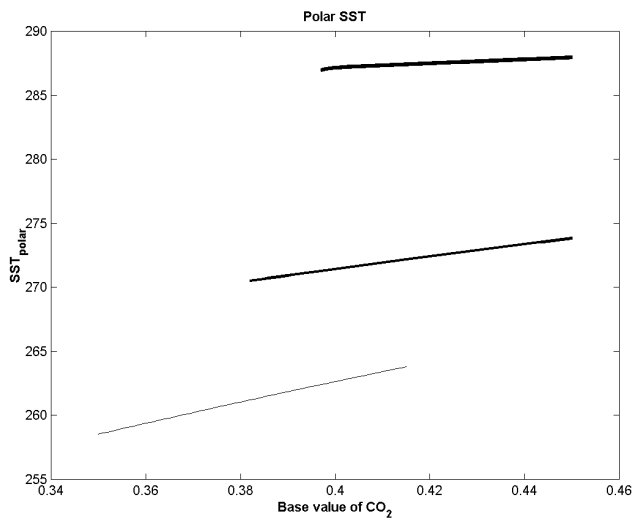

Figure 11. As in Figure 2b, except that insolation is constant and the base value of CO_2 (arbitrary units) is varied (abscissa).

regime. (For example, insufficient incoming solar radiation will keep the model in the cold regime even when other parameters are varied over reasonable ranges.) An example is shown in Figure 11, in which the base value of atmospheric CO_2 (C in equation (8); note that units are arbitrary) has been varied, holding insolation fixed.

5. Discussion

[39] The results presented here suggest that when the vertical mixing that drives the oceans' thermohaline circulation is allowed to be a strong function of the climate state, and when other more conventional feedbacks are included, the steady state climate may fall into two or three regimes distinguished principally by the relative importance of oceanic and atmospheric poleward enthalpy transport. In the hot regime, intense hurricane activity drives a strong poleward enthalpy flux by the oceans, even in the face of a weak meridional temperature gradient; in this model the oceanic enthalpy flux is so strong as to shut down the atmospheric circulation. This is an appealing potential explanation for very warm climates such as that of the early Eocene, when tropical species could be found at very high latitudes, and bottom waters were as much as 15°C warmer than at present [*Zachos et al.*, 2001]. The sensitive dependence of oceanic poleward heat flux on vertical mixing in the Tropics provides a mechanism for driving strong poleward heat flux in the face of weak meridional temperature gradients. It is also consistent with the observed comparative insensitivity of tropical climate. Any effect that acts to cool the Tropics will usually diminish tropical cyclone activity, resulting is diminished vertical mixing and decreased oceanic enthalpy flux out of the Tropics. In the present model, this negative feedback is strong enough to keep tropical temperatures within a relatively narrow range. Conversely, the dependence of oceanic enthalpy transport on hurricane activity destabilizes high-latitude climate.

[40] Periodic forcing, such as orbital forcing, can produce a large response in this model, provided that it induces regime transitions. This would help explain why the earth's climate is so sensitive to the small changes in insolation caused by varying orbit while at the same time remaining stable over very long time periods, during which solar output is thought to have changed by about 30%.

[41] One appealing feature of the existence of multiple stable climate regimes is that they imply that as forcing is varied, transitions from one regime to another will be comparatively sudden, with strong hysteresis in the regime transitions. In this model, the longest explicit timescale is associated with the thermal inertia of the ocean. Given the scaling provided in the Appendix, the thermal timescale of the upper ocean is on the order of 100 days, so that the equilibration timescale of the model is of this order. It must be pointed out, however, that much is missing from the time-dependent dynamics of this model. For example, during a transition to higher temperature, the upper ocean might be expected to adjust quickly, with the warming of the deep ocean occurring over a much longer timescale. Although the latter might affect the timescale of adjustment of atmospheric CO_2, the thermal adjustment of the atmosphere is tied only to the upper ocean response. However, during a transition to lower temperature, the high-latitude ocean must cool through most of its depth, owing to vertical mixing by convection, and thus a considerably longer timescale is implied. By this reasoning, there should also be strong hysteresis in the timescale of warmings versus coolings.

[42] Of potentially greater importance is the effect of transient changes in ocean circulation on the carbon cycle. For example, during a transition from the moderate to hot regime, the high-latitude ocean is flooded with warm water and deep water formation may be expected to cease altogether, with cold bottom water temporarily isolated from the surface until enough vertical mixing and/or geothermal heating occurs to warm the bottom waters and reestablish isopycnal conditions at high latitudes. During this adjustment time, which may last well over 1 kyr, deep vertical mixing would be strongly inhibited by the thermal stratification, possibly affecting the supply of nutrients to surface waters, and thus altering primary productivity. At the same time, depletion of oxygen in the stagnant deep waters by precipitating remains of microorganisms could eventually lead to anoxic conditions in the deep ocean, allowing for greatly increased burial of carbon in deep sea sediments, and consequent increase in atmospheric oxygen content. There is some evidence for the existence of transient deep ocean anoxic events during the Cretaceous, when sapropelic deposits were laid down in the deep ocean [*Ryan and Cita*, 1977]. The abrupt decrease in the bulk sediment deep-sea $\delta^{13}C$ at the onset of the Eocene [*Shackleton*, 1985], coinciding with a rapid climate warming, similarly points to a possible episode of deep ocean anoxia. Strong evidence for episodes of anoxia in Mediterranean coinciding with rapid warming events during the Pleistocene suggest that thermal stratification resulting from rapid warming can indeed lead to anoxia of bottom waters.

[43] One key component of the present model is the strong variation of the partitioning between enthalpy transport by the oceans and atmosphere. Transitions should be accompanied by strong changes in atmospheric circulation. There is considerable paleoclimatological evidence that average wind speeds are inversely correlated with global temperature. Upwelling indices and eolian material in deep-sea cores indicate that average glacial age terrestrial surface winds were between 20 and 50% larger than at present [e.g., see *Janacek and Rea*, 1985] while records of sea salt-derived chloride in ice cores suggests that wind speeds over the North Atlantic and Southern oceans were 50–80% greater. The abrupt warming at the onset of the Eocene was accompanied by a sudden decrease in the mean size of eolian grains in Pacific sediments [*Rea et al.*, 1985]. This is consistent with the present model, in which strong changes in oceanic enthalpy transport are at least partially compensated by changes in atmospheric transport, which is likely correlated with surface wind speed.

[44] Another critical component of the model presented here is the strong dependence of tropical cyclone activity on climate. Unfortunately, very few proxies of past storminess are available to test this important assumption. *Liu and Fearn* [1993] examined sediment cores from nearshore lakes around the Gulf of Mexico and were able to detect sand layers resulting from storm over-wash deposits. While this technique appears to be a reliable indicator of hurricanes near the lake sites, currently available data does not extend as far back as the last ice age. *Brandt and Elias* [1989] show that there is some correlation between the thickness and extent of tempestite deposits and proxies of atmospheric CO_2, suggesting that the intensity and/or frequency of severe oceanic storms was greater during warm periods such as the late Cretaceous. It is not inconceivable that storm proxies could be developed that would allow an assessment of hurricane activity during glacial periods, permitting a test of a principal cornerstone of the present work.

[45] It may be argued that the existence of multiple stable regimes in this model is an artifact of the limited number of degrees of freedom. In future work, we will attempt to explore this issue using models with many degrees of freedom and with better physics and chemistry, including ice-albedo feedback and a more reasonable formulation of the carbon cycle.

Appendix A: Model Equations and Parameter Values

[46] For notational compactness and to reduce the number of control parameters, we first nondimensionalize the model dependent and independent variables, according to Table A1.

[47] In Table A1, T_{eA} is the effective emission temperature of Box A, σ is the Stefan-Boltzmann constant, g is the acceleration of

Table A1. Scaling Factors

Quantity	Scale Factor
All temperatures	T_{eA}
All vertical fluxes, and ocean flux	σT_{eA}^4
Horizontal velocity in atmosphere	$\frac{gL\sigma T_{eA}^3}{C_p \Delta p}$
Time	$\frac{C_p \Delta p}{gL\sigma T_{eA}^3}$

gravity, L is the horizontal distance between the centers of the boxes, C_p is the heat capacity at constant pressure of air, and Δ_p is the pressure thickness of the two atmospheric layers (assumed equal).

[48] Using these scaling factors, the nondimensional model equations are

$$\frac{\partial T_{A2}}{\partial t} = -2\varepsilon_{A2} T_{A2}^4 + \varepsilon_{A2}\varepsilon_{A1} T_{A1}^4 + \varepsilon_{A2}(1-\varepsilon_{A1}) T_{AS}^4 + F_{A2} \tag{A1}$$

$$\frac{\partial T_{A1}}{\partial t} = -2\varepsilon_{A1} T_{A1}^4 + \varepsilon_{A2}\varepsilon_{A1} T_{A2}^4 + \varepsilon_{A1} T_{AS}^4 + F_{A1} - F_{A2} - U(T_{A2} - T_{B1} + \Gamma) \tag{A2}$$

$$\chi \frac{\partial T_{AS}}{\partial t} = 1 + \varepsilon_{A1} T_{A1}^4 + \varepsilon_{A2}(1-\varepsilon_{A1}) T_{A2}^4 - T_{AS}^4 - F_{A1} - F_O \tag{A3}$$

$$\frac{\partial T_{B2}}{\partial t} = -2\varepsilon_{B2} T_{B2}^4 + \varepsilon_{B2}\varepsilon_{B1} T_{B1}^4 + \varepsilon_{B2}(1-\varepsilon_{B1}) T_{BS}^4 + F_{B2} + U(T_{A2} - T_{B2}) \tag{A4}$$

$$\frac{\partial T_{B1}}{\partial t} = -2\varepsilon_{B1} T_{B1}^4 + \varepsilon_{B2}\varepsilon_{B1} T_{B2}^4 + \varepsilon_{B1} T_{BS}^4 + F_{B1} - F_{B2} + U(T_{B2} - T_{B1} + \Gamma) \tag{A5}$$

$$\chi \frac{\partial T_{BS}}{\partial t} = T_{eB}^4 + \varepsilon_{B1} T_{B1}^4 + \varepsilon_{B2}(1-\varepsilon_{B1}) T_{B2}^4 - T_{BS}^4 - F_{B1} - F_O. \tag{A6}$$

[49] In equations (A1)–(A6), U is the atmospheric horizontal transport velocity, and

$$\chi \equiv \frac{\rho_l h_0 C_l g}{C_p \Delta p},$$

$$\Gamma \equiv \frac{g h_0}{C_p T_{eA}},$$

where ρ_l is the density of seawater, h_0 is an average depth of the thermocline, and C_l is the heat capacity of seawater.

[50] The atmospheric transport velocity in equations (A1)–(A6) is given by the nondimensional equivalent of equation (5):

$$U = \beta(T_{A2} - T_{B2} - \Delta T_c), \tag{A7}$$

while the emissivities are given by equation (6):

$$\varepsilon_{i,j} = 1 - e^{-\mathrm{CO}_2 - \gamma q_{i,j}}. \tag{A8}$$

[51] Here the specific humidities are given by their saturation values based on the temperatures, multiplied by a relative humidity H, except that the specific humidity at level 2 in Box B is given by

$$\varepsilon_{B2} = \mathrm{H}\, q_{B2}^*(1 - aU). \tag{A9}$$

[52] Note that the relative humidity, H, can be absorbed into the parameter γ. The carbon dioxide concentration in equation (A8) is given by the nondimensional equivalent of equation (8):

$$\mathrm{CO}_2 = C + \lambda\,(T_{BS} + h(T_{AS} - T_{BS})), \tag{A10}$$

where now λ contains the temperature scaling factor. The vertical convective fluxes that appear in equations (A1)–(A6) are given by the nondimensional equivalent of equation (4):

$$F_{i,j} = \beta\big(T_{i,j} - T_{i,j+1} - \Delta T_{i,j}\big), \tag{A11}$$

where here β is a nondimensional number and $\Delta T_{i,j}$ is based on a moist adiabat and thus depends on $T_{i,j}$. The condition $F_{i,j} \geq 0$ is rigorously enforced.

[53] The ocean enthalpy flux is given by the nondimensional equivalent of equation (1):

$$F_O = D P^{2/3} (T_{AS} - T_{BS})^{2/3}, \tag{A12}$$

where D is a nondimensional constant. According to equations (10) and (14), $P^{2/3}$ in equation (A12) is given by

$$P^{2/3} \sim \varepsilon_T \frac{F_{A1}}{\sqrt{u_*^2 + U^2}}, \tag{A13}$$

where u_* is now a nondimensional gust factor. The parameter ε_T is equation (A13) is unity (its actual value being absorbed into the definition of D), unless F_{A2} is zero, in which case its value is also zero.

[54] Finally, the thermocline depth, h, that appears in equation (A10) is given by the nondimensional equivalent of equation (2):

$$h = \lambda P^{1/3} (T_{AS} - T_{BS})^{-2/3}, \tag{A14}$$

where Λ is a nondimensional parameter.

[55] This completes the specification of the model. The parameter values used in the control run are listed in Table A2. Note that χ only affects the rate of approach to equilibrium and plays no role in steady state solutions and that the model is insensitive to the value of β as long as it is large.

Table A2. Control Run Parameter Values

Parameter	Control Run Value
χ	2
Γ	0.2
β	100
ΔT_c	0.06
γ	2.2
a	1.5
C	−1.08
λ	1.5
D	0.8
u_*	0.45
Λ	0.63

[56] **Acknowledgments.** This work has benefited considerably from advice given by Karen Bice and an anonymous reviewer, as well as from discussions with Peter Molnar, Carl Wunsch, Ed Boyle, Jeff Scott, Peter Stone, and Matthew Huber.

References

Adams, J. M., M. Maslin, and E. Thomas, Sudden climate transitions during the Quaternary, *Prog. Phys. Geogr.*, *23*, 1–36, 1999.

Bice, K. L., and J. Marotzke, Numerical evidence against reversed thermohaline circulation in the warm Paleocene/Eocene ocean, *J. Geophys. Res.*, *106*, 11,529–11,542, 2001.

Bister, M., and K. A. Emanuel, Dissipative heating and hurricane intensity, *Meteor. Atmos. Phys.*, *50*, 233–240, 1998.

Boyle, E. A., and L. D. Keigwin, North Atlantic thermohaline circulation during the past 20,000 years linked to high-latitude surface temperature, *Nature*, *330*, 35–40, 1987.

Brandt, D. S., and R. J. Elias, Temporal variations in tempestite thickness may be a geologic record of atmospheric CO_2, *Geology*, *17*, 951–952, 1989.

Broecker, W. S., D. M. Peteet, and D. Rind, Does the ocean-atmosphere system have more than one mode of operation?, *Nature*, *315*, 21–26, 1985.

Chamberlin, T. C., On a possible reversal of deep-sea circulation and its influence on geologic climates, *J. Geol.*, *14*, 363–373, 1906.

Emanuel, K. A., On thermally direct circulations in moist atmospheres, *J. Atmos. Sci.*, *52*, 1529–1534, 1995.

Emanuel, K. A., A statistical analysis of tropical cyclone intensity, *Mon. Weather Rev.*, *128*, 1139–1152, 2000.

Emanuel, K. A., The contribution of tropical cyclones to the oceans' meridional heat transport, *J. Geophys. Res.*, *106*, 14,771–14,782, 2001.

Goody, R. M., and Y. L. Yung, *Atmospheric Radiation: Theoretical Basis*, 519 pp., Oxford Univ. Press, New York, 1995.

Hall, M. M., and H. Bryden, Direct estimates and mechanism of ocean heat transport, *Deep Sea Res.*, *29*, 339–359, 1982.

Held, I. M., and A. Y. Hou, Nonlinear axially symmetric circulations in a nearly inviscid atmosphere, *J. Atmos. Sci.*, *37*, 515–533, 1980.

Henderson-Sellers, A., H. Zhang, G. Berz, K. Emanuel, W. Gray, C. Landsea, G. Holland, J. Lighthill, S.-L. Shieh, P. Webster, and K. McGuffie, Tropical cyclones and global climate change: A post-IPCC assessment, *Bull. Am. Meteorol. Soc.*, *79*, 19–38, 1998.

Huber, M., and L. C. Sloan, Warm climate transitions: A general circulation modeling study if the late Paleocene Thermal Maximum (~56 Ma), *J. Geophys. Res.*, *104*, 16,633–16,655, 1999.

Imbrie, J., A theoretical framework for the Pleistocene ice ages, *J. Geol. Soc. London*, *142*, 417–432, 1985.

Janacek, T. R., and D. K. Rea, Quaternary fluctuations in the northern hemisphere trade winds and westerlies, *Quat. Res.*, *24*, 150–163, 1985.

Jeffreys, H., On fluid motions produced by differences of temperature and humidity, *Q. J. R. Meteorol. Soc.*, *51*, 347–356, 1925.

Keigwin, L. D., G. A. Jones, and S. J. Lehman, Deglacial meltwater discharge, North Atlantic deep circulation, and abrupt climate change, *J. Geophys. Res.*, *96*, 16,811–16,826, 1991.

Lehman, S. J., and L. D. Keigwin, Sudden changes in North Atlantic circulation during the last deglaciation, *Nature*, *356*, 757–762, 1992.

Liu, K.-B., and M. L. Fearn, Lake-sediment record of late Holecene hurricane activities from coastal Alabama, *Geology*, *21*, 793–796, 1993.

MacDonald, A., and C. Wunsch, The global ocean circulation and heat flux, *Nature*, *382*, 436–439, 1996.

Manabe, S., and P. J. Stouffer, Two stable equilibria of a coupled ocean-atmosphere model, *J. Clim.*, *1*, 841–866, 1988.

Marotzke, J., and J. R. Scott, Convective mixing and the thermohaline circulation, *J. Phys. Ocean.*, *29*, 2962–2970, 1999.

Marotzke, J., and J. Willebrand, Multiple equilibria of the global thermohaline circulation, *J. Phys. Ocean.*, *21*, 1372–1385, 1991.

Munk, W., and C. Wunsch, Abyssal recipes II: Energetics of tidal and wind mixing, *Deep Sea Res.*, *45*, 1977–2010, 1998.

Nilsson, J., and K. A. Emanuel, Equilibrium atmospheres of a two-column radiative convective model, *Q. J. R. Meteorol. Soc.*, *125*, 2239–2264, 1999.

Paillard, D., The timing of Pleistocene glaciations from a simple multiple-state climate model, *Nature*, *391*, 378–381, 1998.

Pearson, P. N., P. W. Ditchfield, J. Singano, K. G. Harcourt-Brown, C. J. Nicholas, R. K. Olsson, N. J. Shackleton, and M. A. Hall, Warm tropical sea surface temperatures in the Late Cretaceous and Eocene epochs, *Nature*, *413*, 481–487, 2001.

Pierrehumbert, R. T., Thermostats, Radiator fins, and the local runaway greenhouse, *J. Atmos. Sci.*, *52*, 1784–1806, 1995.

Rea, D. K., S. A. Hovan, and T. R. Janacek, Geologic approach to the long-term history of atmospheric circulation, *Science*, *227*, 721–725, 1985.

Rind, D., and M. Chandler, Increased ocean heat transports and warm climate, *J. Geophys. Res.*, *96*, 7437–7461, 1991.

Ryan, W. B. F., and M. B. Cita, Ignorance concerning episodes of ocean-wide stagnation, *Mar. Geol.*, *23*, 197–215, 1977.

Sandstrom, J. W., Dynamische Versuche mit Meerwasser, *Ann. Hydrodyn. Mar. Meteorol.*, p. 6, 1908.

Schneider, E. K., B. P. Kirtman, and R. S. Lindzen, Tropospheric water vapor and climate sensitivity, *J. Atmos. Sci.*, *56*, 1649–1658, 1999.

Shackleton, N. J., Oceanic carbon isotope constraints on oxygen and carbon dioxide in the Cenozioc atmosphere, in *The Carbon Cycle and Atmospheric CO_2: Natural Variations Archean to Present*, *Geophys. Monogr. Ser.,* vol. 32, edited by E. T. Sundquist and W. S. Broecker, pp. 412–418, AGU, Washington, D. C., 1985.

Sigman, D. M., and E. A. Boyle, Glacial/interglacial variations in atmospheric carbon dioxide, *Nature*, *407*, 859–869, 2000.

Spencer, R. W., and W. D. Braswell, How dry is the tropical free troposphere? Implications for global warming theory, *Bull. Am. Meteorol. Soc.*, *78*, 1097–1106, 1997.

Wang, X., P. H. Stone, and J. Marotzke, Poleward heat transport in a barotropic ocean model, *J. Phys. Ocean.*, *25*, 256–265, 1995.

Zachos, J. C., L. D. Scott, and K. G. Lohmann, Evolution of early Cenezoic marine temperatures, *Paleoceanography, 9*, 353–387, 1994.

Zachos, J. C., M. Pagini, L. Sloan, E. Thomas, and K. Billups, Trends, rhythms and aberrations in global climate, *Science*, *292*, 686–693, 2001.

K. Emanuel, Program in Atmospheres, Oceans, and Climate, Massachusetts Institute of Technology, Cambridge, MA 02139, USA.